

# Effect of particle size and humidity on sugarcane bagasse combustion in a fixed bed furnace

## Efecto del tamaño de particular y la humedad sobre la combustión de bagazo de caña en un horno de lecho fijo

Zamir Sánchez Castro; Paola Gauthier-Maradej; Humberto Escalante Hernández\*

Centro de Estudios e Investigaciones Ambientales (CEIAM). Universidad Industrial de Santander (UIS), Cr 27 Calle 9, Bucaramanga, Colombia.  
\*escala@uis.edu.co

*Fecha Recepción: 13 de septiembre de 2013*  
*Fecha Aceptación: 21 de noviembre de 2013*

---

### Abstract

The *panela* industry is one of the most important Agro Industries in Colombia, making it the largest per-capita consumer and the second largest producer worldwide. The fuel used in this process is traditionally the sugarcane bagasse (SB) which is a byproduct of milling. However, due to the low efficiency of *panela* furnaces additional fuel is required such as wood, used rubber tires and coal. The fixed-bed furnaces inefficiency is mainly due to incomplete combustion of SB caused by the influence of process variables. Therefore, the aim of this work was to study the influence of particle size (PS) and moisture content (MC) over the combustion stages of SB in fixed-bed furnaces. A three-level factorial design was proposed for PS and MC of SB where the temperature and gas concentration were considered as response variables to evaluate the furnace performance. The results obtained in this work show that if the MC increases then the SB yield in the combustion is decreased. On the other hand, the increasing PS can counteract the effect of the MC of SB.

**Keywords:** *Sugarcane bagasse combustion, influence of particle size, influence of moisture, temperature profiles, concentrations profiles.*

### Resumen

La agroindustria panelera es una de las más importantes en Colombia, convirtiéndolo en el primer consumidor per cápita y segundo productor a nivel mundial. El combustible utilizado en el proceso ha sido tradicionalmente el bagazo de caña (SB) subproducto de la molienda. Sin embargo, debido a las bajas eficiencias de los hornos paneleros se requiere de combustibles adicionales como leña, caucho de llanta y carbón. Gran parte de la ineficiencia de los hornos de lecho fijo se debe a una combustión incompleta del SB, ocasionada por la influencia de las variables del proceso. Por lo anterior, el objetivo de este trabajo fue estudiar la influencia de las variables tamaño de partícula (PS) y contenido de humedad (MC) sobre las etapas de combustión del SB en hornos de lecho fijo. Se planteó un diseño factorial de experimentos con tres niveles para el PS y el MC del SB, donde la temperatura y la concentración del gas de combustión fueron consideradas como variables de respuesta para evaluar el desempeño del horno. Los resultados obtenidos muestran que el incremento del MC ocasiona una reducción en el rendimiento de la combustión del SB. Por otra parte, el incremento en el PS puede contrarrestar el efecto del MC del SB.

**Palabras clave:** *combustión de bagazo de caña, influencia tamaño de partícula, influencia humedad, perfiles de temperatura, perfiles de concentración.*

## Introduction

The sugarcane plant (*Saccharum officinarum L.*) grows in areas with altitudes between 300 and 1800m above sea level, these conditions provide high luminosity and an ambient temperature between 25 and 27°C. Recently, Colombia has approximately 250000 hectares of sugarcane crops for *panela* production with an efficiency of 60 t/ha [1].

The *panela* is a product commercialized in blocks (10cm x 8cm x 3cm) obtained from unrefined sweetener from sugarcane syrup. The stems of the sugarcane plant are cut and transported every 12 months from corps to sugarcane mills, where they are crushed. As a result, a juice (syrup) and a residual by-product called sugarcane bagasse (SB) are obtained. The juice is subjected to evaporation, and it is concentrated until a 94wt% of sugar, to produce the *panela*. SB corresponds to approximately 40wt% of the total stem mass [1]. Thus, Colombia has an average SB production about 6x10<sup>6</sup>t/year. The SB is stored in sheds at environmental conditions of temperature and pressure and is used as fuel in the furnaces [2]. Worldwide, the use of agricultural waste as a renewable energy source has become a technological alternative to mitigate the greenhouse effect [3].

The average elemental composition of SB (mass fraction) is 49.27% carbon, 42.87% oxygen, 5.67% hydrogen, 1.67% ash and traces of nitrogen and sulfur, with Lower Heat Value (LHV) of 19.37 MJ/kg dry mass basis [4]. Even when the chemical composition of SB is similar to wood [5], with a combustion yields in fixed bed higher than 90% [6], in Colombia, the sugarcane furnaces uses only 30 to 40% of chemical potential energy of SB and the energy loss reaches 10% by incomplete combustion and 40% by unreacted material. For this reason, the Colombian sugarcane industry uses other fuels (wood, coal and used rubber tires), causing a negative environmental impact and increasing production costs [7].

The efficiency of biomass combustion process is affected by the particle size and moisture content. The thermal decomposition of wood residues in form of blocks [8] and log [9] has shown that increasing the particle size causes an overlapping during the stages of drying, pyrolysis and char oxidation, thereby increasing the burning times. However, Gort (1995) and Rönnbäck *et al.* (2000) (Cited by Yang *et al.* [10]) found that increasing particle size during fixed-bed combustion of biomass stimulates

the combustion rates and therefore enhances the power supplied to the furnace. Meanwhile, during SB combustion in suspended furnaces, it has found that increasing the particle size causes variation in the heat released due to some material is accumulated on the grate before reacting [11].

The moisture content of biomass affect the fuel quality, as it reduces its LHV, combustion temperature [12] and causes difficulty in ignition and instability during the process [13]. The biomass drying consumes large amount of energy to the moisture evaporation. The moisture content in the residue hinders homogeneous heating and leads to the overlapping of combustion stages [8] and increasing of conversion time [14]. The energy consumption for biomass drying during fixed-bed combustion causes a reduction in the propagation rate of combustion fronts [15].

The combustion efficiency of biomass in fixed bed can be determined from temperature profiles and gas concentration. Records of fuel temperature in bed allow to indirectly determining the combustion rate [16]. The peak temperature in the furnace provides information about the sensible heat of flue gas [17], which is used for evaporation of sugarcane juice. The concentration of CO<sub>2</sub> and CO in flue gas indicates the conversion degree of carbon in the biomass [18]. The concentration of flue gas and the oxidation reactions allow a balance to determining the amount of energy released.

Traditionally in Colombia, the *panela* industry uses SB, with particle sizes greater than 50 mm, as fuel for their furnaces [19], and a moisture between 30 and 45wt% [2]. Currently, the influence of these operating variables in the combustion process is unknown. Therefore, the objective of this research was to study the influence of particle size (PS) and the moisture content (MC) of SB on combustion efficiency. The energy efficiency of biomass in fixed-bed furnaces for *panela* production was evaluated from the performance of the combustion rate, the maximum temperatures obtained and the average concentration of CO and CO<sub>2</sub> in flue gas.

### Combustion of a biomass particle

During the biomass combustion, a stagnant film of gas is formed around the particle in which the mass and energy transport phenomena and oxidation reactions are held. The biomass combustion involves three stages: moisture evaporation, devolatilization (thermal decomposition) and char oxidation [15].

During the biomass combustion, drying is controlled by mass and heat transport [20]. Increasing of

velocity and temperature of the gas mixture (steam and combustion products) improves mass transfer and heat coefficient, and increasing the evaporation rates [21]. The evaporation rate is controlled initially by capillary transport and when the water, present in pores of the residue, is evaporated the diffusion phenomenon controls the process [22].

According to the physicochemical composition of biomass, the thermal decomposition stage begins between 200°C [23] and 250°C [11] and ends between 500°C [24] and 600°C [25]. This stage is controlled by the heat transfer to the particle [26]. During the thermal decomposition, volatile gases are released (CO, CO<sub>2</sub>, H<sub>2</sub>, CH<sub>4</sub> and small amounts of tars) and char is produced [27]. The volatiles react with oxygen between 400 and 600°C producing the flame [23]. Combustion intensity and flame length is a function of the gas temperature and the mixing rate (turbulence) [28].

The char oxidation stage has three regimes: i) at temperatures between 350 and 620°C is controlled by intrinsic kinetics, ii) at the temperature range between 640 and 870°C is controlled by both intrinsic kinetics as the oxygen diffusion and iii) at temperatures above 875°C, oxidation kinetics

is higher than oxygen diffusion and the reaction occurs on the surface of the particle [29]. When combustion is controlled by intrinsic kinetics, large amount of O<sub>2</sub> diffuses into the particle to produce CO<sub>2</sub>. If the diffusion and intrinsic kinetics are comparable, both CO as CO<sub>2</sub> are produced on the surface of the particle. In the diffusion controlled regime O<sub>2</sub> is rapidly consumed to produce CO, which reacts with the oxygen in the gas film reducing its concentration. Subsequently, the greatest amount of CO<sub>2</sub> formed returns to the surface and it is again reduced to CO [30].

**Biomass combustion in fixed beds**

Figure 1 shows a characteristic temperature profile during biomass combustion in a fixed-bed furnace. When the biomass ignition starts on the bed surface the drying, devolatilization and char oxidation stages occur as fronts, that propagating in countercurrent with primary air stream. The heat transferred from the flame, by both convection and radiation, to the fresh biomass layers allows drying and devolatilization of the material. The volatiles released and the char formed are produced by exothermic reactions that allowing stable propagation of fronts [31].

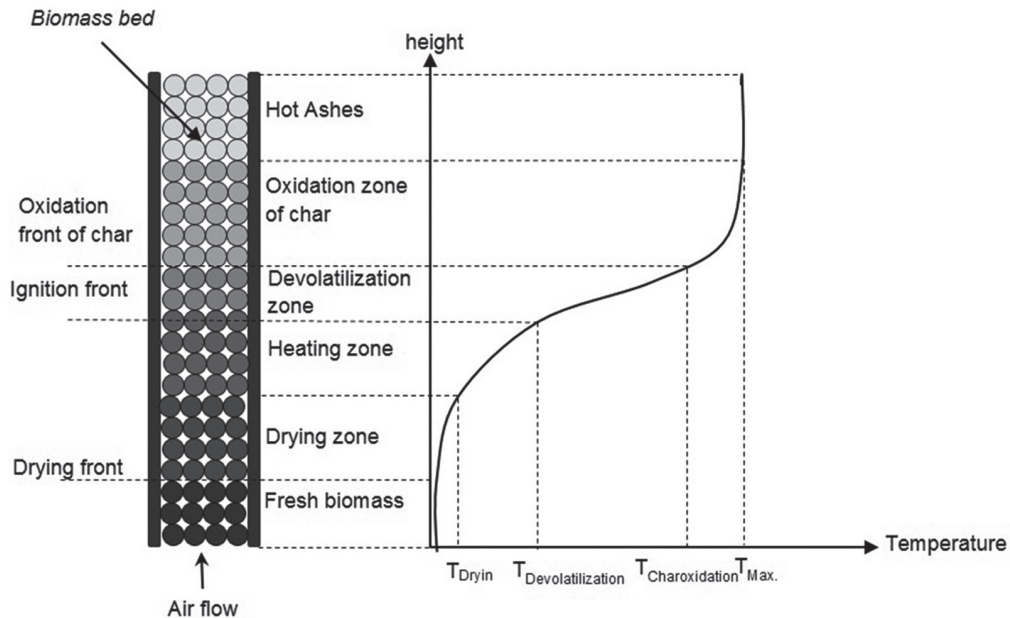


**Figure 1.** Fronts of drying, ignition and char oxidation during biomasses combustion in fixed bed.

Because there are the volatiles oxidation and flame, the devolatilization front is called “ignition front” [15] or “flame front” [16]. Each front is influenced by both the particle size [32] as the fuel humidity [18]. Depending on operating conditions, biomass combustion in fixed-bed with air supply through

a grate, leads to the process fronts propagate in sequentially or simultaneously form [15]. During biomass combustion with small particle sizes, heat transfer by internal conduction is faster than heat transfer by external convection. These combustion processes are characterized by an

isothermal behavior and sequential combustion stages [33]. During biomass combustion with large particle sizes (pellets, briquettes and logs), internal temperature gradients are high and lead to simultaneous combustion stages [8]. For this reason, the velocity of combustion front (sum of drying, ignition and char oxidation) and the operating temperature are likely to increase with the particle diameter [9]. The studies about combustion of wood [34] and straw [16] in fixed-bed furnaces report a reduction in the propagation rate of combustion front by increasing the particle size between 3 and 30mm. However, for combustion of municipal solid waste, increasing the particle size between 10 and 30mm, leads to an increase in the propagation rate of fronts [10].

Agricultural biomass has high concentrations of volatile material (mass fractions above 70wt%) [3], and therefore the combustion rate ( $r_c$ ) is defined from the propagation velocity of biomass ignition front ( $v_f$ ) and the initial bulk density of bed ( $\rho_a$ ) [16] as shown in Equation 1.

$$r_c = v_f \cdot \rho_a \quad (1)$$

As temperature records in bed allow determining the combustion rate, the propagation velocity of biomass ignition front can be obtained from the model proposed by [17] as shown in Equation 2.

$$v_f = \frac{\Delta s}{\Delta t} \quad (2)$$

Where  $\Delta s$  is the distance between two adjacent temperature measurement and  $\Delta t$  is the time required for the front moves in this distance.  $\Delta t$

is directly obtained from the temperature versus time profile, as shown in Figure 2 for the drying front. The determination of fronts of ignition and char oxidation follows the same procedure used to drying front, taking as reference temperatures 400 [23] and 650°C [29], respectively.

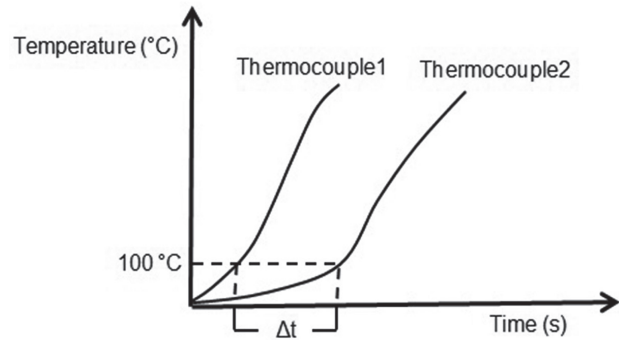


Figure 2. Determination of  $\Delta t$  from the temperature profile.

### Methodology

SB combustion was carried out in a fixed bed furnace (0.3m x 0.3m x 2.23m) with refractory brick walls 0.2m thick, coated by thermal insulating glass fiber (Figure 3). The furnace has two air inlets, a primary flow is fed through the grate and a secondary flow is supplied through two orifices of 0.05 m in diameter. The primary and secondary air flows were maintained at 0.54kg/(m<sup>2</sup>.s) and 0.84kg/(m<sup>2</sup>.s), respectively, and are supplied by two centrifugal fans with variable power.

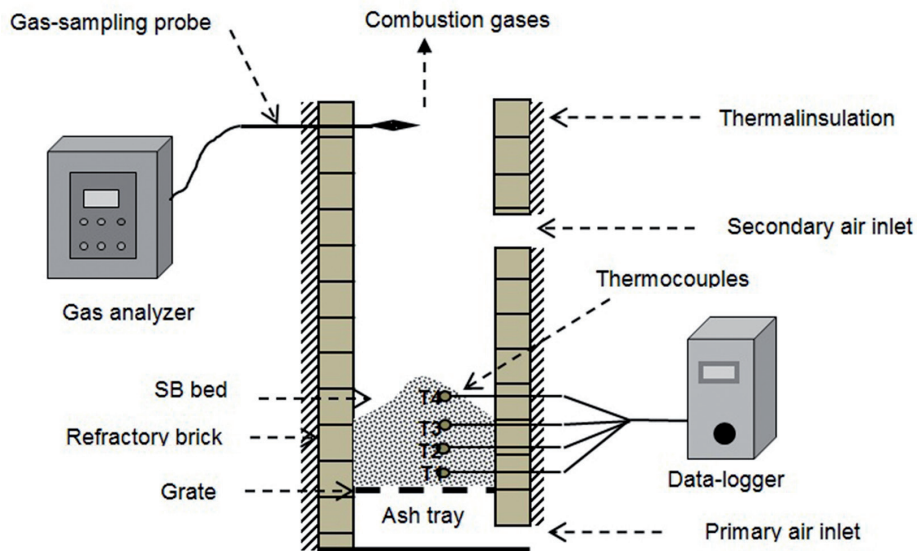


Figure 3. Fixed bed furnace for SB combustion.

Temperatures in the furnace are recorded by four thermocouples, K-type *Instrumatic* brand, axially located at a distance of 0.1m between them and 0.15m depth in bed. The thermocouples are numbered sequentially from the bottom to top of the bed and connected to a data-logger to store the temperature values every 10s. The flue gas composition is determined at the furnace outlet, using a portable analyzer 350 XL TESTO brand which reads online every 5s. The propagation velocity of each front was evaluated by Equation 2, using  $\Delta S = 0.1\text{m}$ . Each temperature range in bed allowed calculating a punctual velocity of the combustion fronts. The overall propagation rate of each front is calculated as an average of the punctual velocities. The combustion rate was evaluated by Equation 1.

The SB was collected in a sugarcane mill in Barbosa city in the Santander Department (Colombia, 05°55'57" N and 73°37'16" W). The SB was dried at ambient conditions of temperature and pressure to achieve MC of 10, 30 and 42wt%. Subsequently, SB was reduced in size using a hammer mill 51001 Farm King brand to obtain particles with cylindrical shape (20mm of length). Then the SB particles were classified through standard sieves (ASTM E-11/95) allowing the separation of particles by their size in 5.0, 3.5 and 1.0mm. SB combustion was made in batch operation and the ignition of the bed was performed on the surface, providing direct fire.

The maximum bed temperature was taken as an average of the peaks recorded by the four thermocouples. The heating rate, for each temperature measurement point, was calculated using Equation 3.

$$\text{Heat Rate} = \frac{(T_{env} - T_{peak})}{t} \quad (3)$$

Where  $T_{env}$  is the environmental temperature,  $T_{peak}$  is the peak temperature and  $t$  is the time necessary to achieve the  $T_{peak}$ . Therefore, the heating rate of the bed is the average of the four measurements performed in the test. To evaluate the effect of PS and MC, a  $3^2$  factorial design was structured, which led to perform nine experiments (Table 1), with their duplicates.

**Table 1.** Experimental design for PS and MC analysis.

Experiment	PS (mm)	MC (%)	SB load (kg)	Bulk density (kg/m <sup>3</sup> )
1	1.0	10	1.7	51.21
2	3.5	10	1.7	42.22
3	5.0	10	1.7	31.47
4	1.0	30	2.1	65.84
5	3.5	30	2.1	54.27
6	5.0	30	2.1	40.46
7	1.0	42	2.6	79.46
8	3.5	42	2.6	65.50
9	5.0	42	2.6	48.83

## Results and Discussion

### Concentration and temperature gas profiles during SB combustion

Figure 4 shows the temperature profiles in the bed. The development of the combustion front are observed, which are propagated from top to bottom of the bed, accompanied by an increase in temperature. Initially, the heat emitted from the ignition source allows drying and devolatilizing of SB particles on the bed surface. The volatiles and char produced react with the primary air flow. All experiments reached a maximum temperature in the interval between 700 to 1000°C.

SB combustion with MC less than 42wt% in all PS levels studies show a sequential increase in temperature from top (T4) to the bottom (T1) of the bed at shorter combustion time, indicating the propagation of combustion front. In fact, in according with Figure 4, the SB combustion begins in the top (T4) where, initially, the temperature is higher than the other zones. Then, the propagation of combustion front allows an increase of the temperature of the other zones, sequentially, (from T3 to T4) to reach the maximum temperature in the bed. A particularly case is presented for SB combustion with MC of 42wt% where is observed an overlapping of temperatures T2 and T3 for PS

from 1.0 to 3.5mm, and T3 and T4 for PS of 5.0mm. An increase in the MC allows raising the heat consumed during the drying stage and causing that the bed temperature is maintained near 100°C for a longer time, slowing its elevation. This moisture effect leads to the formation of irregular combustion front (not flat), as evidenced by the superposition of the bed temperatures (Figure 4). The study about combustion of straw showed that the formation of irregular combustion front generates a large amount of unburned material in the bed [35]. Thus, SB combustion with 42wt% of MC is not recommended.

For SB with PS of 1.0mm and MC at 30 and 42wt% was showed the formation of two temperature peaks. In the Figure 4, the first peak is reached before 900s and second peak after 1000s. Simulations of straw

combustion in fixed bed performed by Zhou *et al.* [16] show the formation of two areas in the furnace: an intense combustion zone and a preheating zone. For the case of SB testing the first peak in temperature is attained when the combustion fronts reach the thermocouple T1 (located 10cm above the grate), indicating intense combustion zone. The last 10cm of the furnace operate as a preheating zone, where much of the heat released in the combustion front is transferred to the primary air flow which enters at 25°C; this causes an initial bed cooling. However, the O<sub>2</sub> concentration in the preheating zone is close to atmospheric value (21vol%), which allows an increase in oxidation rates of volatile and char, releasing more heat than the transferred to the primary air. For this reason is observed a second temperature peak.

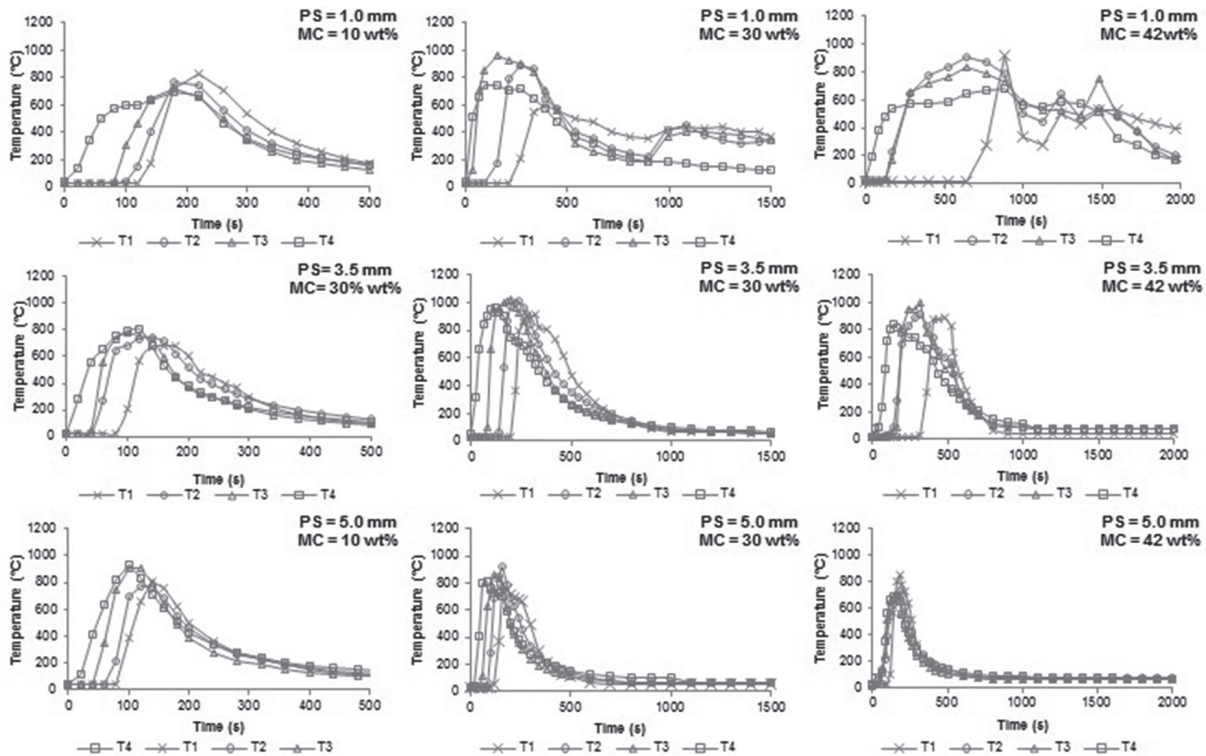


**Figure 4.** Temperature profiles in the bed vs time for PS and MC studied.

The effect of the preheating zone is not observed in the temperature profiles for PS of 5.0 and 3.5mm, nor for PS of 1.0mm with 10wt% MC. During combustion of biomass the increase in particle size reduces the specific surface area of the bed (m<sup>2</sup>/m<sup>3</sup>) [36], which reduces the heat transferred to the primary air and therefore the cooling of the bed. Moreover, for the PS of 1.0mm the increase in the heat lost by evaporation with MC over 10wt%,

causes a greater susceptibility to be cooled by the primary air.

Combustion of very humid biomass requires more time to evaporate the water, involves delaying the start of the devolatilization step and therefore increases the overall process time. For example, during the combustion of municipal solid waste, the MC increased from 30 to 50wt% causes an increase in process time between 65 [18] to 140%

[37]. During all the experiments of SB combustion, the MC in the residue caused delays in the arrival of the fronts to the bottom of bed, inducing an increase in processing time. The increase in PS during SB combustion tests counteracted the effect of MC on the combustion time. For a SB with PS of 1.0mm, MC increased from 10 to 30wt% results in increased

burning time of 117% and for SB with PS of 3.5 and 5.0mm the increase was 100 and 50%, respectively. The PS influence on SB combustion is evidenced by representing the heating rate of the bed as a function of PS and MC (Figure 5). For SB in a MC determined, the increase in PS allows to a higher heating rate.

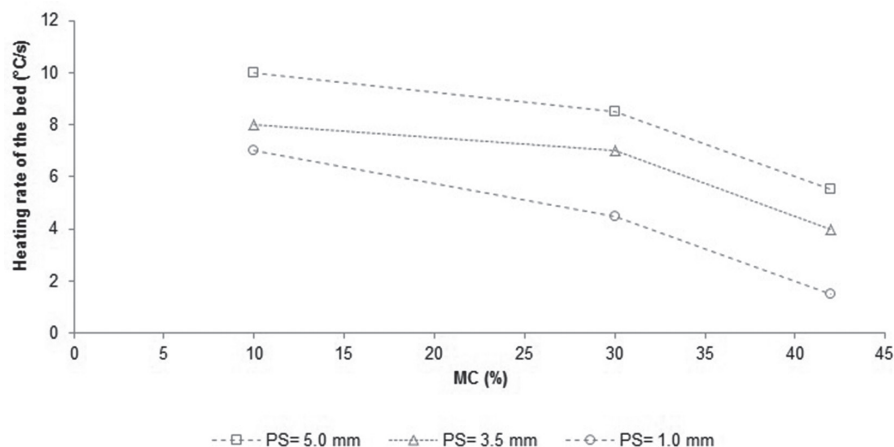


**Figure 5.** Heating gradients of the bed as a function of PS and MC studied.

The increase in PS leads to a reduction of the bulk bed density (Table 1), which results in an increase in the bed porosity. A high value of porosity favors the radiation penetration into the bed and increases the residence time of flue gas [38]. For this reason, increasing the PS of the SB bed favors the heating rate as indicated by Figure 5. These results are consistent with those reported by Yang *et al.* [10], who found that an increase in the bed porosity between 0.3 and 0.5 enhancing the combustion rate; the bed porosity of BS is greater than these. The heating rate of the SB bed has a tendency inversely proportional to the water content in the biomass due to increased heat lost during evaporation. However, the humidity effect is less strong for MC below 30wt%. Comparing temperature profiles (Figure 4) it can be noted that, for the three PS, the maximum temperature is registered for SB combustion with MC of 30wt%, increasing the heat transfer from the reaction zone to fresh SB layers.

Figure 6 shows the behavior of CO and CO<sub>2</sub> concentrations as function of time during SB combustion. The increase in CO and CO<sub>2</sub> concentrations is proportional to the decrease in oxygen concentration due to oxidation of the carbon present in the biomass. During SB combustion, the maximum CO fraction (4.9vol%) was obtained with PS of 5.0mm and MC of 42wt%, indicating that these operating conditions has the highest energy

losses by incomplete combustion and unburned material (as indicated above). Moreover, the greater CO<sub>2</sub> concentration (17vol%) was reported with PS of 5.0mm and 10wt% MC, indicating that a biomass with low MC favors the combustion process. Moreover, the greater CO<sub>2</sub> fraction (17vol%) was reported with PS of 5.0mm and 10wt% MC, indicating that a biomass with low MC favors the combustion process.

Table 2 presents a summary of the burning time, the maximum bed temperature and the mean concentration of flue gas for SB combustion with different PS and MC.

Zhou *et al.* [16] showed that the increase in MC enlarges the drying time and decreases the rate of volatile released, allowing a lot of oxygen can be react with the char. When MC increases from 10 to 30wt%, it is observed that for SB combustion of different PS, initially the maximum bed temperature rises. However, for MC above 30wt% the additional heat released by char oxidation is consumed during the evaporation, reducing the maximum bed temperature. This behavior is in agreement with the results found for corn straw combustion where the maximum temperature was obtained for a residue with MC of 32wt% [17]. The average recorded temperature range (from 760 to 980°C) is within the reported interval for other biomass such as pinewood [5] and municipal solid waste [18] with MC between 10 and 49wt%.

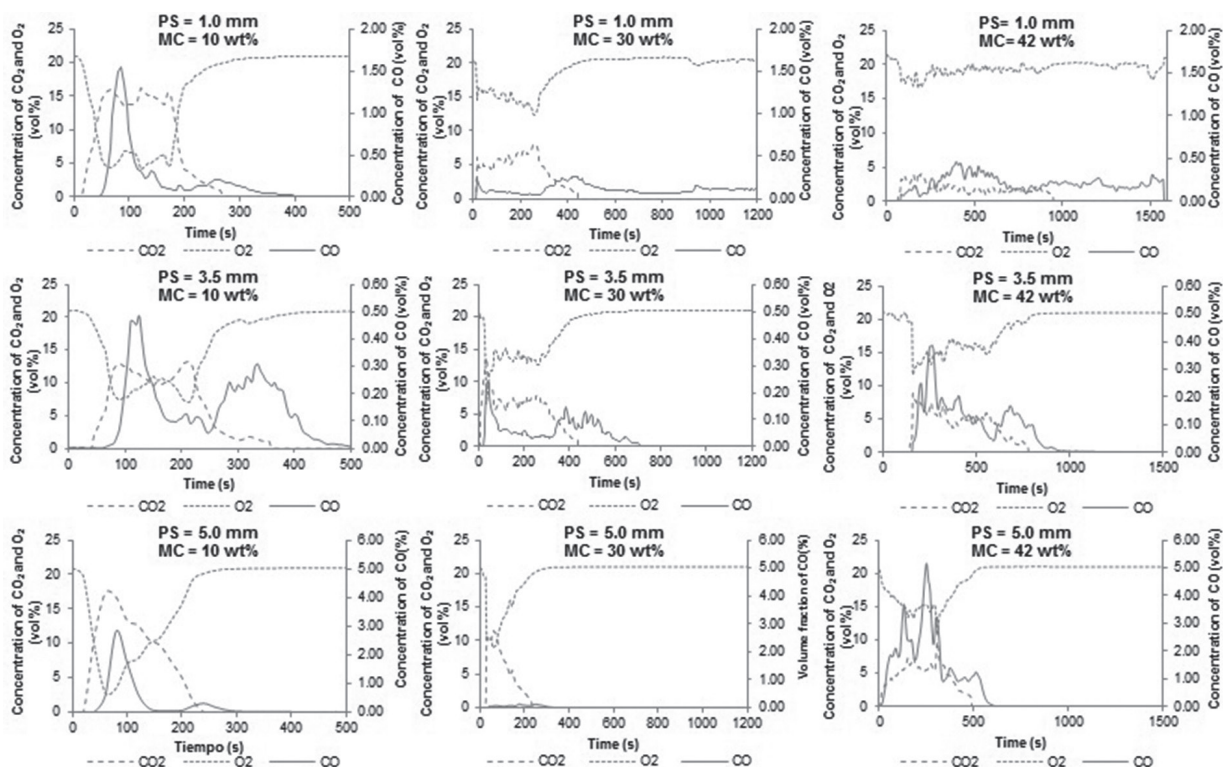


Figure 6. CO<sub>2</sub>, O<sub>2</sub> and CO concentration profiles Vs time for different PS for the MC studied.

Table 2. Burning time, maximum average temperature in the bed and average gas concentration during SB combustion.

PS (mm)	MC (%)	Burning time (s)	Maximum bed temperature (°C)	Mean concentration of the flue gas (vol%)		
				CO <sub>2</sub>	O <sub>2</sub>	CO
1.0	10	120	780	10.00	10.32	0.31
1.0	30	260	870	4.71	16.05	0.12
1.0	42	720	850	1.94	19.00	0.15
3.5	10	100	760	10.15	10.24	0.16
3.5	30	200	980	5.85	14.86	0.07
3.5	42	340	920	4.53	16.25	0.23
5.0	10	80	860	10.20	10.33	0.61
5.0	30	120	890	6.10	14.62	0.08
5.0	42	----	700	4.79	15.97	1.98

SB, with high MC, have great burning times due to slow consumption rate of carbon in biomass, which is reflected in the reduction of the CO<sub>2</sub> concentration in the flue gas. SB combustion with 10wt% of MC showed CO<sub>2</sub> concentration close to 10vol%, while

for 30wt% of MC, this volumetric fraction was around 5.5%. Moreover, SB combustion with 42wt% of MC showed a CO<sub>2</sub> concentration in a wider range, with volume fractions between 1.94 and 4.79%. The results of this investigation are according with



results of the simulation of municipal solid waste combustion, in a fixed bed. These studies reported that a MC variation from 10 to 49wt% leads to reduction in the CO<sub>2</sub> concentration from 7.88 to 4.17vol% [18].

The increase in MC from 10 to 30wt% causes a decrease in the CO concentration due to the reduction in the combustion rate. Later, when MC increases to 42wt% CO concentration increases again. Daood *et al.* [29], in their thermogravimetric studies of SB, determined that the decreasing in temperature reduces the char oxidation rate. This effect and the increased processing time highlight the low performance of SB combustion at MC above 42wt%. The CO<sub>2</sub> concentration showed a

directly proportional behavior to PS, confirming that the increase in PS improves combustion efficiency. A similar proportionality between the CO<sub>2</sub> concentration and PS was found during combustion of pinewood [5].

**Propagation velocity of drying fronts, ignition and char oxidation**

Figure 7 shows the propagation velocity of drying, ignition and char oxidation fronts during SB combustion calculated from Equation 2. Behavior is shown only for SB experiments with MC lower than 42wt%, since this moisture to the combustion process showed the lowest performance as was explained before.

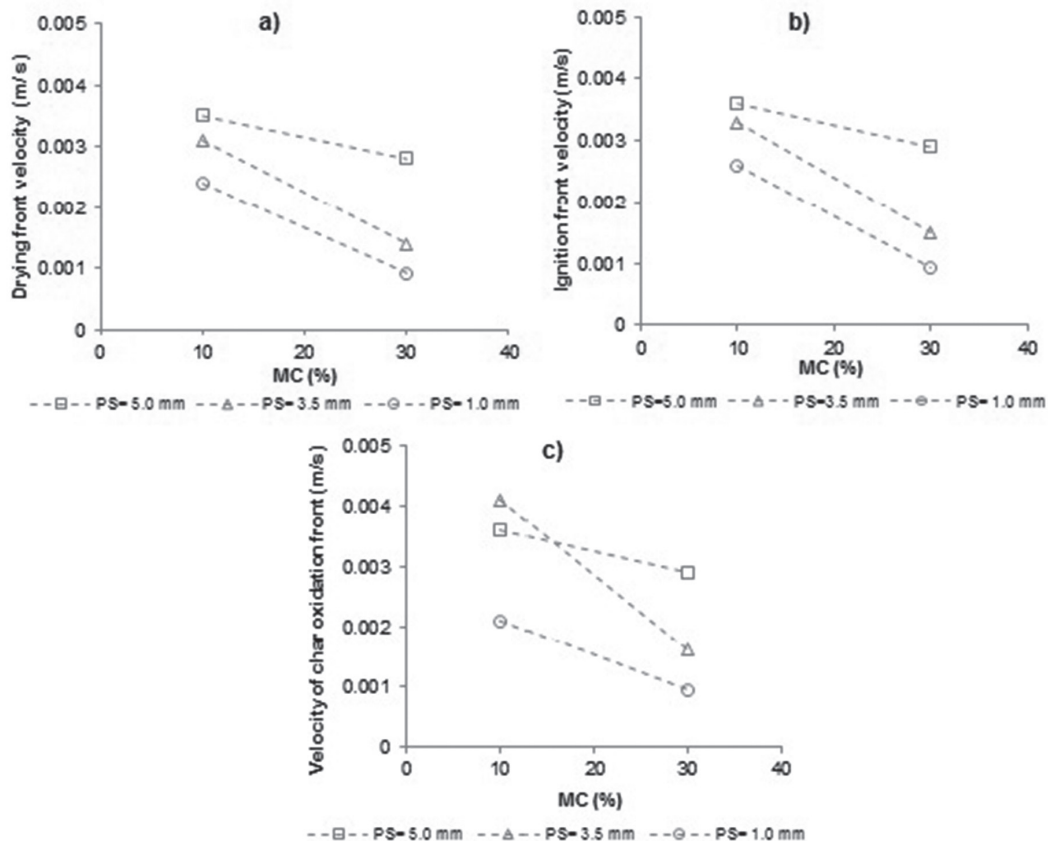


**Figure 7.** Propagation velocities of fronts: a) Drying, b) Ignition c) Char Oxidation, depending on PS and MC studied.

The propagation velocity of the three fronts is reduced during SB combustion processes, with the use of high MC. This must be because the increase in MC in the SB fibers reduces the release of volatiles and their oxidation rate [17] which, in addition to the increased heat required for evaporation, leads to a decrease of the energy released in the reaction zone. Therefore,

the heat transferred from the flame to the subsequent layers of biomass decays, reduces the propagation velocity of drying, ignition and char oxidation fronts. Nevertheless, lower slopes were found with PS of 5.0mm, indicating that MC has low effect on SB combustion of this size; this behavior is consistent with the trend of heating rate (Figure 5).

During SB combustion, the drying and ignition stages (Figure 7a and 7b) have a similar behavior in function of PS and MC. The propagation velocity of these fronts is favored by increasing PS, as a consequence of a higher heating of the bed (Figure 5). The char oxidation stages (Figure 7c) shows a different behavior to the above stages with respect to PS. He *et al.* [39] determined, during a study of coal-particles combustion, that the oxidation rate does not

follow a linear behavior with respect to PS and it has its highest value at a given particle diameter, according to the temperature conditions in the furnace. Consequently, for BC with low MC (10%wt) the highest propagation front of char's oxidation is obtained to 3.5mm. While for BC with MC of 30%wt, the highest propagation front of char's oxidation is obtained to 5.0mm. Figure 8 shows the combustion rate of SB dry basis, calculated from Equation 1.

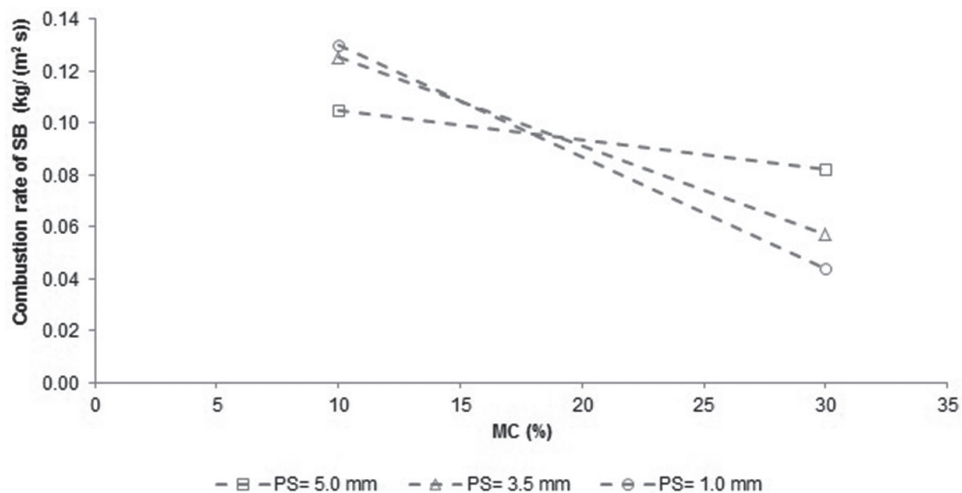


**Figure 8.** Combustion rate of SB on a dry basis.

In according to Figure 8, the increase in MC reduces the SB combustion rate for the three PS analyzed. This behavior is a direct consequence of the declining propagation velocity of the ignition front. However, when MC increases from 10 to 30wt%, the decrease in the combustion rate is only 18% for 5.0mm of PS, whereas for lower PS, it was higher than 55%. This confirms that the increase in PS favors SB combustion. The SB combustion rates obtained in this work are in the range of other biomass such as municipal solid waste [18], rice straw [16, 34] and almonds palm oil [40], with MC between 10 and 30wt%.

The biomass combustion rate is a function of both the propagation velocity of ignition front and the bulk density of the bed (Equation 1). For SB with 10wt% of MC, the combustion rate showed an inversely proportional behavior to PS, while for 30wt% of MC, the behavior was directly proportional. The SB combustion with 10wt% of MC has a small decrease in the propagation velocity of the ignition front when the PS decreases. This was counteracted by increasing the bulk density of the bed (Table 1) causing an increase

in the combustion rate. Similar results were found during wood combustion in fixed bed with humidity values around 10wt% [15]. Nonetheless, for SB with 30wt% of MC, the propagation velocity of the ignition front decreases strongly with the reduction of PS and reduced the combustion rate.

### Statistical analysis

The analysis of variance (ANOVA) was realized to determine the influence of PS and MC on the response variables: combustion rate and average concentration of  $\text{CO}_2$ , during SB combustion. This analysis was done using the statistical software *Statgraphics Centurion* with a confidence level of 95%. The results are presented in Tables 3 and 4. Table 3 shows that PS, MC and its interaction cause significant effects on the combustion rate. The p-value demonstrates that the smallest influence is caused by PS while the greatest influence is due to the interaction between PS and MC. These results corroborate the behavior found in Figures 5, 7 and 8. Table 4 shows that the effect of PS and MC as well as their interaction are active on the average concentration of  $\text{CO}_2$ .

The p-value indicates that the variables have a similar significance. However, the variation in the concentration of CO<sub>2</sub> with change in the MC is different for the different levels of PS, having the greatest influence with PS of 1.0mm as evidenced in Table 2.

**Table 3.** Influence of PS and MC on combustion rate.

Source	Sum of squares	df	Mean square	F-ratio	p-value
A:PS	0.009408	1	0.009408	7.19	0.0213
B:MC	0.0156963	1	0.0156963	12.00	0.0053
AA	0.0149654	1	0.0149654	11.44	0.0061
AB	0.0905251	1	0.0905251	69.20	0.0000
BB	0.0100668	1	0.0100668	7.70	0.0181
blocks	0.00366939	1	0.00366939	2.80	0.1221
Total error	0.0143899	11	0.00130817		
Total (corr.)	0.158721	17			

**Table 4.** Influence of PS and MC on average concentration of CO<sub>2</sub>.

Source	Sum of squares	df	Mean square	F-ratio	p-value
A:PS	7.05333	1	7.05333	114.23	0.0000
B:MC	124.099	1	124.099	2009.85	0.0000
AA	1.6384	1	1.6384	26.53	0.0003
AB	3.79501	1	3.79501	61.46	0.0000
BB	7.75623	1	7.75623	125.62	0.0000
blocks	0.000672222	1	0.000672222	0.01	0.9188
Total error	0.679199	11	0.0617453		
Total (corr.)	145.022	17			

## Conclusions

During SB combustion the heat consumed in the drying stage reduces the combustion rate and CO<sub>2</sub> concentration and increases CO concentration. Therefore, the combustion process efficiency is enhanced using MC lower than 30wt% of SB. The SB combustion efficiency also is favored when the heating rate of the bed is increased, which is achieved by using residues with large particle sizes, that facilitates the heat penetration by radiation and greater residence time. For this reason, the increase in PS of SB counteracts the effect of MC, allowing both higher combustion rates and higher CO<sub>2</sub> concentration. The best operation conditions during combustion of SB in fixed bed are achieved with a PS of 5.0mm and 10wt% of MC. In the other hand, SB combustion with MC of 30wt% had the highest average temperatures caused by better char combustion during the devolatilization

stage. The panela's agroindustry use BS with MC of 50% and PS no homogeneous. To achieve a SB with MC of 10% in a short time is necessary an artificial drying process, which increase the operating costs. Therefore is recommended to panela's agroindustry the use of SB with PS of 5.0mm and MC of 30wt% for achieve a better performance of the combustion of SB.

## Acknowledgements

The authors are grateful to Corporación Colombiana de Investigación agropecuaria (CORPOICA) for providing the necessary resources for this investigation, as well as the facilities for performing the tests. Also to Universidad Industrial de Santander (UIS) and its Centro de Estudios e investigaciones Ambientales (CEIAM), for their support in the analysis of results.

## References

- [1] García HR, Albarracín LC, Toscano A, Santana NJ, Insuasty O. Guía tecnológica para el manejo integral del sistema productivo de caña panelera. Colombia: Produmedios editorial para el sector agropecuario; 2007.
- [2] Gordillo G, García HR. Manual para el diseño y operación de hornillas paneleras. Colombia: Corpoica; 1992.
- [3] Demirbas A. Combustion characteristics of different biomass fuels. *Prog Energ Combust.* 2004;30(2):219-30.
- [4] Escalante H, Orduz J, Zapata HJ, Cardona MC, Duarte M. Atlas del potencial energético de la biomasa residual en Colombia. Colombia: Ediciones Universidad Industrial de Santander; 2011.
- [5] Yang YB, Ryu C, Khor A, Sharifi VN, Swithenbank J. Fuel size effect on pinewood combustion in a packed bed. *Fuel.* 2005;84(16):2026-38.
- [6] Yin C, Rosendahl LA, Kaer SK. Grate-firing of biomass for heat and power production. *Prog Energ Combust.* 2008;34(6):725-754.
- [7] García HR. Desarrollo de modelos demostrativos de hornillas de alta eficiencia térmica y bajo impacto ambiental de acuerdo con los niveles socioeconómicos y técnicos de las principales regiones productoras de panela en Colombia: final report. Bogotá: Corpoica; 2011.
- [8] Bryden MK, Hagge MJ. Modeling the combined impact of moisture and char shrinkage on the pyrolysis of a biomass particle. *Fuel.* 2003;82(13):1633-44.
- [9] Galgano A, Di Blasi C. Modeling the propagation of drying and decomposition front in wood. *Combust Flame.* 2004;139(1-2):16-27.
- [10] Yang YB, Ryu C, Khor A, Yates NE, Sharifi VN, Swithenbank J. Effect of fuel properties on biomass combustion. Part II. Modelling approach—identification of the controlling factors. *Fuel.* 2005;84(16):1039-46.
- [11] Shanmukharadhya KS. Simulation and thermal analysis of effect of fuel size on combustion in an industrial biomass furnace. *Energ Fuel.* 2007;21(4):1895-900.
- [12] Werther J, Saenger M, Hartge E-U, Ogada T, Siagi Z. Combustion of agricultural residues. *Prog Energ Combust.* 2000;26(1):1-27.
- [13] Woodfield LP, Kent JH, Dixon TF. Computational modeling of combustion instability in bagasse-fired furnaces. *ExpTherm Fluid Sci.* 2000;21(1-3):17-25.
- [14] Sand U, Sandberg J, Larfeldt J, Bel Fdhila R. Numerical prediction of the transport and pyrolysis in the interior and surrounding of dry and wet wood log. *Appl Energ.* 2008;85(12):1208-24.
- [15] Porteiro J, Patiño D, Collazo J, Granada E, Moran J, Miguez JL. Experimental analysis of ignition front propagation of several biomass fuels in a fixed-bed combustor. *Fuel.* 2010;89(1):26-35.
- [16] Zhou H, Jensen AD, Glarborg P, Jensen PA, Kavaliuscas A. Numerical modeling of straw combustion in a fixed bed. *Fuel.* 2005;84(4):389-03.
- [17] Zhao W, Li Z, Zhao G, Zhang F, Zhu Q. Effect of air preheating and fuel moisture on combustion characteristics of corn straw in a fixed bed. *Energ Convers Manage.* 2008;49(12):3560-5.
- [18] Liang L, Sun R, Fei J, Wu S, Liu X, Dai K, et al. Experimental study of effects of moisture content on combustion characteristics of simulated municipal solid waste in a fixed bed. *Bioresource Technol.* 2008;99(15):7238-46.
- [19] Soler JP, Gómez FH. Determinación de los parámetros de diseño y operación de cámaras de combustión tipo Ward-Cimpa en hornillas paneleras, (proyecto de grado). Bucaramanga: Universidad industrial de Santander; 2004.
- [20] Bennamoun L, Belhamri A. Mathematical description of heat and mass transfer during deep bed drying: Effect of product shrinkage on bed porosity. *Appl Therm Eng.* 2008;28(17-18):2236-44.
- [21] Lerman P, Wennberg O. Experimental method for designing a biomass bed dryer. *Biomass Bioenerg.* 2011;35(1):31-9.
- [22] Wang ZH, Chen G. Heat and mass transfer in batch fluidized-bed drying of porous particles. *Chem Eng Sci.* 2000;55(10):1857-69.
- [23] Ramajo-Escalera B, Espina A, García JR, Sosa-Arno JH, Nebra SA. Model-free Kinetics applied to sugarcane bagasse combustion. *Thermochim Acta.* 2006;448(2):111-6.
- [24] Katyal S, Thambimuthu K, Valix M. Carbonisation of bagasse in a fixed bed reactor: influence of process variables on char yield and characteristics. *Renew Energ.* 2003;28(5):713-25.
- [25] Asadullah M, Rahman MA, Ali MM, Rahman MS, Motin MA, Sultan MB *et al.* Production

- of bio-oil from fixed bed pyrolysis of bagasse. *Fuel*. 2007;86(16):2514-20.
- [26] Zabaniotou A, Damartzis Th. Modeling the intra-particle transport phenomena and chemical reactions of olive kernel fast pyrolysis. *J Anal Appl Pyrol*. 2007;80(1):187-94.
- [27] Di Blasi C. Modeling chemical and physical processes of wood and biomass pyrolysis. *Prog Energ Combust*. 2008;34(1):47-90.
- [28] Frigerio S, Thunman H, Leckner B, Hermansson S. Estimation of gas phase mixing in packed bed. *Combust Flame*. 2008;153(1-2):137-48.
- [29] Daood SS, Munir S, Nimmo W, Gibbs BM. Char oxidation study of sugar cane bagasse, cotton stalk and Pakistani coal under 1% and 3% oxygen concentrations. *Biomass Bioenerg*. 2010;34(3):263-71.
- [30] Basu P. Combustion of coal in circulating fluidized-bed boilers: a review. *Chem Eng Sci*. 1999;54(22):5547-57.
- [31] Kausley SB, Pandit AB. Modelling of solid fuel stoves. *Fuel*. 2010;89(3):782-91.
- [32] Johansson R, Thunman H, Leckner B. Influence of intraparticle gradients in modeling of fixed bed combustion. *Combust Flame*. 2007;149(1-2):49-62.
- [33] Bryden MK, Ragland KW. Numerical modeling of a deep, fixed bed combustion. *Energ Fuel*. 1996;10(2):269-75.
- [34] Thunman H, Leckner B. Influence of size and density of fuel on combustion in a packed bed. *P Combust Inst*. 2005;30(2):2939-46.
- [35] Khor A, Ryu C, Yang Y, Sharifi VN, Swithenbank J. Straw combustion in a fixed bed combustor. *Fuel*. 2007;86(1-2):152-60.
- [36] Lu H, Ip E, Scott J, Foster P, Vickers M, Baxter L. Effects of particle shape and size on devolatilization of biomass particle. *Fuel*. 2010;89(5):1156-68.
- [37] Yang YB, Ryu C, Goodfellow J, Sharifi VN, Swithenbank J. Modeling waste combustion in a grate furnaces. *Process Saf Environ*. 2004;82(B3):208-22.
- [38] Rohsenow WM, Hartnett JP, Cho YI. *Handbook of heat transfer*. 3<sup>rd</sup> Ed. United State of America: McGraw Hill; 1998.
- [39] He R, Suda T, Fujimori T, Sato Jun'ichi. Effects of particle sizes on transport phenomena in single char combustion. *Int J Heat Mass Tran*. 2003;46(19):3619-27.
- [40] Razuan R, Chen Q, Zhang X, Sharifi V, Swithenbank J. Pyrolysis and combustion of oil palm stone and palm kernel cake in fixed-bed reactors. *Bioresource Technol*. 2010;101(12):4622-9.